1987, *65*, 1804. (b) Harrod, J. F.; Yun, S. S. *Organometallics* **1987**, *6*, 1381. (c) Aitken, C.; Barry, J.-P.; Gauvin, F.; Harrod, J. F.; Malek, A.; Rousseau, D. *Organometallics* **1989**, *8*, 1732. (d) Harrod, J. F.; Ziegler, T.; Tschinke, V. *Organometallics* **1990**, *9*, 897. (e) Woo, H.-G.; Harrod, J. F.; Henique, J.; Samuel, E. *Oraganometallics* **1993**, *12*, 2883. (f) Britten, J.; Mu, Y.; Harrod, J. F.; Polowin, J.; Baird, M. C.; Samuel, E. *Organometallics* **1993**, *12*, 2672. (g) Xin, S.; Woo, H.-G.; Harrod, J. F.; Samuel, E.; Lebuis, A.-M. *J. Am. Chem. Soc.* **1997**, *119*, 5307. (h) Gauvin, F.; Harrod, J. F.; Woo. H.-G. *Adv. Organomet. Chem.* **1998**, 43.

7. (a) Woo, H.-G.; Tilley, T. D. *J. Am. Chem. Soc.* **1989**, *111*, 3757. (b) Woo, H.-G.; Tilley, T. D. *J. Am. Chem. Soc.* **1989**, *111*, 8043. (c) Woo, H.-G.; Heyn, R. H.; Tilley, T. D. *J. Am. Chem. Soc.* **1992**, *114*, 5698. (d) Woo, H.-G.; Walzer, J. F.; Tilley, T. D. *J. Am. Chem. Soc.* **1992**, *114*, 7047. (e) Woo, H.-G.; Walzer, J. F.; Tilley, T. D. *Macromolecules* **1991**, *24*, 6863. (f) Imori, T.; Woo, H.-G.; Walzer, J. F.; Tilley, T. D. *Chem. Mater.* **1993**, *5*, 1487. (g) Tilley, T. D. *Acc. Chem. Res.* **1993**, *26*, 22.
8. (a) Woo, H.-G.; Kim, S.-Y.; Han, M.-K.; Cho, E. J.; Jung, I. N. *Organomatallics* **1995**, *14*, 2415. (b) Woo, H.-G.; Kim, S.-Y.; Kim, W.-G.; Cho, E. J.; Yeon, S. H.; Jung, I. N. *Bull. Korean Chem. Soc.* **1995**, *16*, 1109. (c) Woo, H.-G.; Song, S.-J.; You, H.; Cho, E. J.; Jung, I. N. *Bull. Korean Chem. Soc.* **1996**, *17*, 475. (d) Woo, H.-G.; Song, S.-J. *Bull. Korean Chem. Soc.* **1996**, *17*, 494.
9. Seyferth, D.; Wood, T. G.; Tracy, H. J.; Robison, J. L. *J. Am. Ceram. Soc.* **1992**, *75*, 1300.
10. Seyferth, D.; Sobon, C. A.; Borm, J. *New J. Chem.* **1990**, *14*, 545.
11. Kim, D.-P.; Lee, J.-D. *Korean J. Mater. Res.* **1996**, *6*, 515.
12. Yajima, S.; Shishido, T.; Okamura, K. *Am. Ceram. Soc. Bull.* **1977**, *56*, 1060.
13. (a) Hadden, N.; Baumann, F.; MacDonald, F.; Munk, M.; Stevenson, R.; Gere, D.; Zamaroni, F.; Majors, R. *Basic Liquid Chromatography*; Varian Aerography, 1971. (b) Krstulovic, A. M.; Brown, P. R. *Reversed-Phase High Performance Liquid Chromatography*; Wiley: New York, 1982.
14. Yajima, S.; Okamura, K.; Hayashi, J. *J. Am. Ceram. Soc.* **1975**, *58*, 1209.
15. Harris, R. K.; Kennedy, J. D.; McFarlane, W. In *NMR and the Periodic Table*; Harris, R. K., Mann, B. E., Eds.; Academic Press: London, 1978; Chapter 10.
16. Woo, H.-G.; Song, S.-J.; Cho, E. J.; Jung, I. N. *Bull. Korean Chem. Soc.* **1996**, *17*, 123.
17. Seyferth, D.; Lang, H. *Organometallics* **1991**, *10*, 551.
18. Wiseman, A. I.; Jones, R. G.; Swain, A. C.; Went, M. J. In *Silicon-Containing Polymers*; Jones, R. G., Ed.; The Royal Society of Chemistry: Cambridge (UK), 1995; p 191.
19. Collman, J. P.; Hegedus, L. S.; Norton, J. R.; Finke, R. G. *Principles and Applications of Organotransition Metal Chemistry*; University Science Books: Mill Valley, California, 1987.
20. Song, S.-J.; Woo, H.-G. Manuscript in preparation.

Molecular Orbital Studies of Bonding Characters of Al-N, Al-C, and N-C Bonds in Organometallic Precursors to AlN Thin Films

Kee Hag Lee*, Sung Soo Park, Han Myoung Lee, Su Jin Park†, Hang Soo Park, Yoon Sup Lee†*, Yunsoo Kim†*, Sehun Kim†*, Chan Gyun Jo, and Heui Man Eun‡

Department of Chemistry, WonKwang University, Iksan 570-749, Korea
†Department of Chemistry and Center for Molecular Science
Advanced Institute of Science and Technology, Taejon 305-701, Korea
‡Advanced Materials Division, Korea Research Institute of Chemical Technology, Taejon 305-600, Korea
‡Department of Chemistry, Kunsan National University, Kunsan 573-369, Korea
Received May 19, 1998

Electronic structures and properties of the organometallic precursors $[Me_2AlNHR]_2$ (R = Me, ^{i}Pr, and ^{t}Bu) have been calculated by the semiempirical (ASED-MO, MNDO, AM1 and PM3) methods. Optimized structures obtained from the MNDO, AM1, and PM3 calculations indicate that the N-C bond lengths are considerably affected by the change of the R groups bonded to nitrogen, but the bond lengths of the Al-N and Al-C bonds are little affected. This result is useful in explaining the experimental results for the elimination of the R groups bonded to nitrogen, and could serve as a guide in designing an optimum precursor for the AlN thin film formation.

Introduction

Aluminum nitride (AlN) exhibits interesting properties for electronic applications (chemical inertness, good thermal stability, piezoelectricity, etc.). The thermal expanesion coefficient of AlN is very similar to that of silicon in the range from room temperature to 200 °C (AlN: 3.5×10^{-6}/K, Si: 3.4×10^{-6}/K). Its flexural strength at room temperature is 5,000 kg/cm^2 which is extremely higher than those of Al_2O_3 (3,100-3,200 kg/cm^2) and BeO (2,500 kg/cm^2).[1] It also has a high

*Address correspondence to these authors.

melting temperature (~2,500 °C).[2] AlN is a wide band gap III-V semiconductor with the hexagonal wurtzite structure. It has a large band gap (6.0-6.5 eV),[3,4] a high electrical resistivity (5×10^{13} cm),[1] and a high thermal conductivity at room temperature (160 W/mK).

By electron spectroscopic study,[5] it has been reported that the valence band of AlN consists mainly of N 2*s* and 2*p* electrons, whereas the conduction band reflects essentially an Al character. Li *et al.* have studied AlN thin films grown by low temperature reactive RF sputter deposition.[6] Here, AlN is revealed to be a promising material for passivation and dielectric layers in semiconductor devices as well as for electronic substrates. Additionally, single crystalline AlN films have potential for applications in high frequency surface acoustic wave (SAW) devices due to their piezoelectric character and high SAW velocity. Moreover, the optical transparency of the film throughout the visible and near-infrared regions, combined with its resistance to chemical attack, makes it potentially useful for optical devices and coatings. Because of its attractive thermal, electronic, and mechanical properties, AlN has received widespread attention in recent years.[7-10]

A general route to nonoxide ceramic materials is the pyrolytic decomposition of a suitable organometallic precursor.[11,12] The single precursor organometallic chemical vapor deposition (OMCVD) has been shown to have a number of important advantages over the conventional CVD process.[12] Thus, amido- and imido-compounds of aluminium have received considerable attention.[13-17] The single precursor OMCVD method using compounds with the Al-N bonds was recently employed.[18-21] The advantage here is that the precursors have both Al and N atoms, and it is relatively easy to control reaction parameters.

For the preparation of the AlN thin films using a single precursor, it is important to understand the decomposition pathway of the Al-N, Al-C, and N-C bonds. Thus, AlN reaction pathway and Al-N bonding characters have been studied.[20,21] In the study of the deposition of AlN using $[Me_2AlNR_2]_2$ compounds,[21] with the change of the alkyl group (^{i}Pr, ^{t}Bu) bonded to N, optimum deposition temperatures were found to differ as follows: the deposition temperatures of bis(dimethyl-μ-isopropylamido-aluminum) (BDPA) and bis(dimethyl-μ-t-butylamido-aluminum) (BDBA) are about 770 K and 720 K, respectively. Also the amount of nitrogen in the film was found to be somewhat larger with BDBA than with BDPA indicating more favorable dissociation of the N-C bonds in the case of BDBA. To the best of our knowledge, no previous theoretical study of the AlN precursors has involved the understanding of the electronic properties and atomic structures.

We have studied the electronic properties and atomic structures of selected precursors by using the semiempirical molecular orbital theories (ASED-MO, MNDO, AM1, and PM3) in order to investigate the bonding characters of the Al-N, Al-C, and N-C bonds. Here selected precursors are *cis*- and *trans*-bis(dimethyl-μ-methylamido-aluminium) (BDMA), BDPA, and BDBA, which have different alkyl groups bonded to N.

Calculations

First, the Atom Superposition and Electron Delocalization-Molecular Orbital (ASED-MO) method[10,22,23] is performed on constrained (idealized) geometries, ensuring that all members of the series have the same bond lengths for the bonds under question, since by doing that it is possible to understand the electronic effect of the alkyl substituents. ASED-MO method is probably the simplest semi-empirical approach capable of predicting molecular structures, binding energies, and electronic properties. The semiempirical ASED-MO theory employs atomic parameters for predicting properties of molecules. This technique[10] has already been used in a study of methane activation by hole sites on AlN. Atomic orbital parameters used in the calculation are listed in Table 1.[10]

Concerning the strength for a bond, the orbital overlap population $OOP_{\mu\nu}$ (E_i) between two atoms is used. For the precursors, $OOP_{\mu\nu}$ (E_i) are discrete values of E_i. But in giving the plots, a Gaussian broadening is made similar to the DOS. The summation of $OOP_{\mu\nu}$ (E_i) over the occupied states gives the bond order, which is not a well-defined quantity, but a very useful chemical description.[24]

The constrained structures of the precursors used in the calculations of electronic properties are based on the X-ray data for BDPA obtained by Amirkhalili *et al.*,[14] which are schematically shown in Figure 1.

Since the coordinates of the H atoms are unobtainable from the X-ray data, the bond lengths of the N-H and C-H bonds are arbitrarily chosen to be 1.00 Å and 1.09 Å, respectively, and all the H atoms bonded to C atoms are placed in staggered conformations.

In addition to the calculations of the constrained geometries derived from the X-ray structures, we optimized the geometries of the precursors in order to understand the effect of alkyl substituents on the structures of the precursors. The calculations were carried out with the MNDO, AM1, and PM3 calculations as implemented in the program package[25] MOPAC93. No symmetry constraints were specified for the geometry optimization.

Results and Discussion

The structures of the precursors used in the calculation are schematically shown in Figure 1. The differences among these precursors are the R groups (Me, ^{i}Pr, ^{t}Bu) bonded to N atoms as shown in the figure.

Electronic properties of the precursors in the constrained geometries are analyzed by the Mulliken population analysis. The reduced overlap populations (ROPs) in Table 2 were

Table 1. Atomic orbital parameters used in the ASED-MO calculations

Atom	Orbital	ζ^a(a.u.)	H_{ii}(eV)
Al	3s	1.5213	− 12.62
	3p	1.5041	− 7.986
N	2s	1.4737	− 18.33
	2p	1.467	− 12.53
C	2s	1.658	− 14.59
	2p	1.618	− 9.2
H	1s	1.2	− 11.6

[a] Slater type orbital exponent.

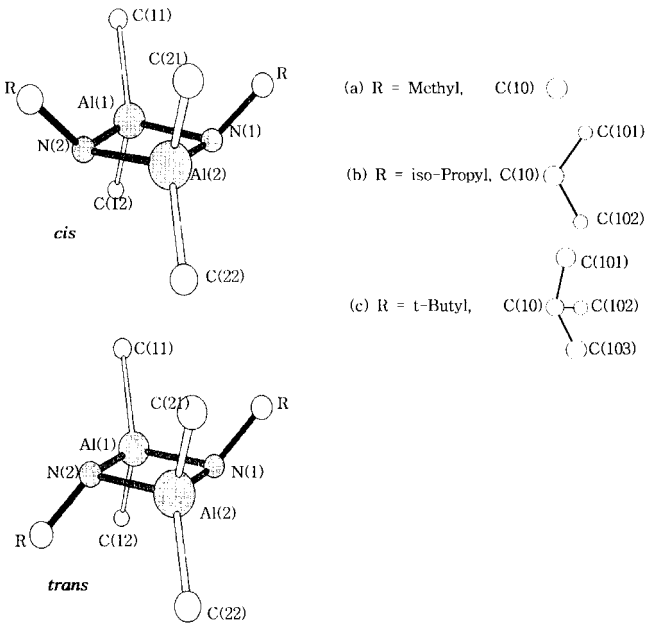

Figure 1. The structures of precursors used in this calculation. The BDMA isomers are the *cis*- and *trans*-$[AlMe_2NHMe]_2$ (a), the BDPA isomers are the *cis*- and *trans*-$[AlMe_2NH^iPr]_2$ (b), and the BDBA isomers are the *cis*- and *trans*-$[AlMe_2NH^tBu]_2$ (c).

calculated by ASED-MO, MNDO, AM1, and PM3 methods with the constrained geometry based on the X-ray structure[14] of *cis*-BDPA. In the ASED-MO calculations, which is not a self-consistent one, electron drifts are somewhat exaggerated. The N-C ROPs increase in the order: *cis*-BDMA < *cis*-BDPA < *cis*-BDBA. The Al-N ROPs also increase in the same order. In the case of Al-C ROPs, neither the Al1-C12 nor the Al2-C22 ROPs are changed. The Al1-C11 and Al2-C21 ROPs each are slightly changed when the R group is changed from Me to ^{i}Pr (0.16% and 0.00% on the basis of BDMA) and when the R group is changed from ^{i}Pr to ^{t}Bu (0.7% and 1.14% on the basis of BDMA).[26] The calculated results, therefore, suggest that the electron donor effect of the R group bonded to N atom is very small on bonds between Al and alkyl group. Here, the ROP means the total overlap population between a pair of atoms to which all occupied orbitals contribute, thus making an inference to bond strength. The ASED-MO and AM1 calculations suggest that the Al-N, N-C, and Al-C bonds may be the strongest in BDBA. The MNDO calculations suggest that the Al-N and Al-C bonds may be the strongest, while the N-C bonds may be the weakest in BDBA. The PM3 calculations suggest that the Al-C and N-C bonds may be the weakest in BDBA. But the MNDO, AM1, and PM3 calculations suggest that those bonds are negligibly changed as shown in Table 2. However, the trends[20] experimentally observed for the decomposition of N-C bonds are not in line with the electronic effect of alkyl substituents.

In order to consider bonding character in the constrained geometries by the ASED-MO method, the decompositions of the bond charge with respect to energy distribution of the Al-N, Al-C, and N-C bonds are plotted in Figure 2 as OOP(E) versus E curve. The OOP peaks distribute right below the Fermi level, and are of bonding nature. Figure 2a shows the Al-N bonding character. BDMA shows a very small antibonding character in the HOMO state, but BDPA and BDBA show bonding character in the HOMO states. The Al-C bond (Figure 2b) reveals hardly any antibonding character in the HOMO states. In the case of N-C, the antibonding character increases in the order: BDMA < BDPA < BDBA (Figure 2c). Changing the R group in the bulky order of Me < ^{i}Pr < ^{t}Bu results in the stabilization of the Al-N bond in HOMO in the order BDMA < BDPA < BDBA, whereas the N-C bond is destabilized in the same order. The interesting result is that the order for a magnitude of antibonding peak for the N-C bonds in the HOMO of ASED calculations is the same as the order of the increasing N-C bond lengths in MNDO, AM1, and PM3 calculations. This may be fortuitous, or may suggest that the OOP of N-C bonds at the HOMO level could represent a lability of bonds with similar ionic character.

The net charges in Table 3 are calculated by the ASED-MO, MNDO, AM1, and PM3 methods for the constrained geometries. The variation of net charges on Al in the ASED-MO and PM3 calculations is little, but that in the MNDO and AM1 calculations shows a slight decrease in size in the order BDMA < BDPA < BDBA. The negative charge on N

Table 2. ROPs of *cis*-$[AlMe_2NHR]_2$ (R=Me, ^{i}Pr, ^{t}Bu) in the constrained geometries calculated by ASED-MO, MNDO, AM1, and PM3 methods

Atom	ASED			MNDO			AM1			PM3		
	BDMA	BDPA	BDBA	BDMA	BDPA	BDBA	BDMA	BDPA	BDBA	BDMA	BDPA	BDBA
Al(1)-N(1)	0.578	0.579	0.584	0.380	0.383	0.385	0.430	0.432	0.433	0.428	0.429	0.424
Al(1)-N(2)	0.587	0.588	0.593	0.382	0.385	0.387	0.431	0.433	0.435	0.427	0.429	0.424
Al(2)-N(1)	0.566	0.567	0.571	0.376	0.379	0.380	0.426	0.427	0.428	0.428	0.429	0.425
Al(2)-N(2)	0.568	0.570	0.574	0.378	0.381	0.382	0.427	0.429	0.430	0.428	0.429	0.425
Al(1)-C(11)	0.614	0.615	0.621	0.622	0.623	0.626	0.636	0.636	0.640	0.491	0.484	0.484
Al(1)-C(12)	0.603	0.603	0.603	0.613	0.614	0.614	0.628	0.628	0.628	0.505	0.501	0.493
Al(2)-C(21)	0.605	0.605	0.609	0.619	0.619	0.621	0.634	0.635	0.637	0.494	0.487	0.483
Al(2)-C(22)	0.614	0.614	0.614	0.616	0.616	0.617	0.629	0.629	0.628	0.494	0.491	0.484
N(1)-C(10)	0.781	0.851	0.884	0.532	0.532	0.531	0.565	0.570	0.571	0.536	0.537	0.535
N(2)-C(20)	0.765	0.830	0.861	0.521	0.521	0.521	0.555	0.560	0.561	0.530	0.532	0.530

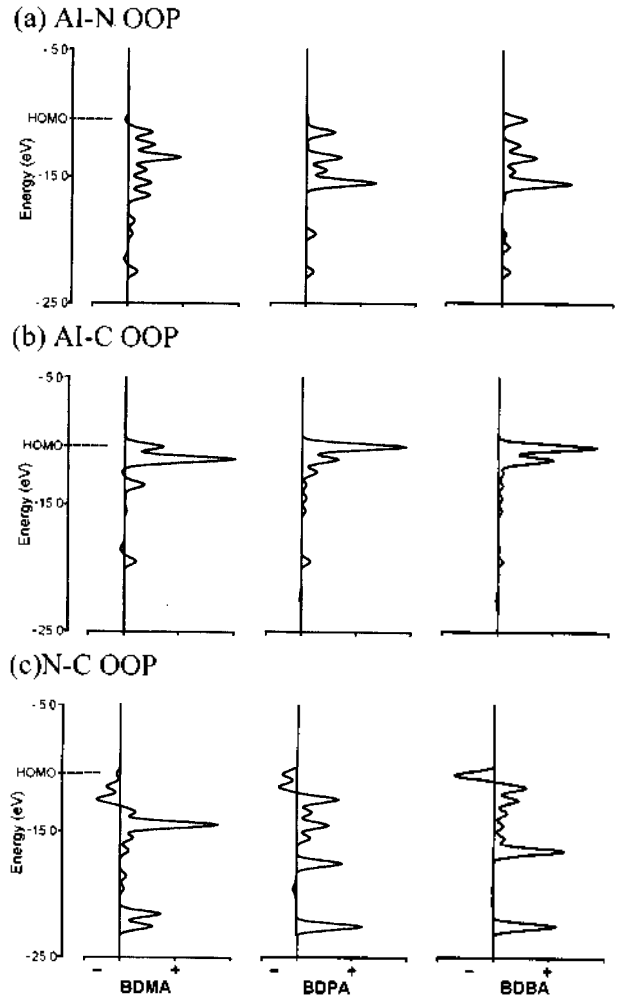

Figure 2. The orbital overlap populations (OOPs) of Al-N (a), Al-C (b), and N-C (c) bonds of *cis* isomers for BDMA, BDPA, and BDBA precursors with the constrained geometries. Dashed lines indicate the HOMO energy levels. Calculations were done by ASED-MO method.

atom in the ASED-MO calculations is shown to increase in the following order: Me < ^{i}Pr < ^{t}Bu, but the values in the MNDO, AM1, and PM3 calculations are in the reverse order. The positive charge on C atom bonded to N atom in the ASED-MO, AM1, and PM3 calculations is shown to increase in the following order: Me < ^{i}Pr < ^{t}Bu, but the MNDO calculations show the reverse order. Changing the R group in the bulky order Me < ^{i}Pr < ^{t}Bu shows that the bond between Al and N in the ASED-MO calculations is polarized in size in the increasing order BDMA < BDPA < BDBA, but that in the MNDO, AM1, and PM3 calculations is reverse. The bond between N and C in the ASED-MO calculations is polarized in size in the increasing order BDMA < BDPA < BDBA, but that in the MNDO, AM1, and PM3 calculations is reverse. The sum of net charge for $(AlN)_2$ fragment in the ASED-MO calculations shows the tendency of decreasing in the order Me < ^{i}Pr < ^{t}Bu, but that in MNDO, AM1, and PM3 is reverse. This discrepancy seems to come from the fact that the ASED-MO method implicitly includes the electron-electron interaction effect, but the MNDO, AM1, and PM3 methods include the parameters for the electron-electron interaction part in their Hamiltonians. Here, our results suggest that it may be difficult to be discernible the electron donor effect, which increases in the order Me < ^{i}Pr < ^{t}Bu in experimental organic chemistry, at the level of MNDO, AM1, and PM3 in our constrained structures.

To understand the steric effect of BDMA, BDPA and BDBA, the MNDO, AM1, and PM3 methods are applied to optimize the geometries for *cis*- and *trans*-isomers of them. In Table 3, we show the MNDO, AM1, and PM3 geometry parameters calculated for BDMA, BDPA, and BDBA, together with the available experimental geometry of BDPA.[14] We note that the MNDO, AM1, and PM3 frequency calculations for the precursors yielded no negative frequencies, thus showing that the reported structures are indeed minima. The numbering system of the atoms in the precursors are shown in Figure 1. The optimized geometry parameters obtained by the MNDO, AM1, and PM3 methods are comparable with the x-ray geometrical parameters of BDPA. The differences in the bond lengths between *cis*- and *trans*-isomers are quite small. In Table 4, the Al-N and Al-C bond lengths in MNDO and AM1 calculations are negligibly changed like the result of ROPs in the ASED-MO, MNDO, AM1, and PM3 methods, but the N-C bond lengths in the MNDO, AM1, and PM3 calculations increase by 0.031 Å, 0.035 Å, and 0.049 Å, respectively, when the R group is changed from Me through ^{i}Pr to ^{t}Bu. Also, the N-C bond lengths in the MNDO, AM1, and

Table 3. Net Charge of *cis*-$[AlMe_2NHR]_2$ (R=Me, ^{i}Pr, ^{t}Bu) in the constrained geometries calculated by ASED-MO, MNDO, AM1, and PM3 methods

Atom	ASED			MNDO			AM1			PM3		
	BDMA	BDPA	BDBA	BDMA	BDPA	BDBA	BDMA	BDPA	BDBA	BDMA	BDPA	BDBA
Al(1)	0.49	0.49	0.49	0.66	0.64	0.64	0.45	0.44	0.43	0.77	0.77	0.77
Al(2)	0.51	0.51	0.51	0.66	0.64	0.64	0.45	0.44	0.43	0.77	0.77	0.77
N(1)	-0.24	-0.26	-0.27	-0.54	-0.51	-0.50	-0.45	-0.43	-0.42	-0.15	-0.14	-0.14
N(2)	-0.25	-0.27	-0.27	-0.54	-0.51	-0.50	-0.45	-0.43	-0.42	-0.16	-0.15	-0.15
C(11)	-0.20	-0.20	-0.21	-0.25	-0.24	-0.24	-0.50	-0.49	-0.49	-0.64	-0.64	-0.66
C(21)	-0.21	-0.21	-0.21	-0.25	-0.25	-0.25	-0.51	-0.50	-0.50	-0.63	-0.63	-0.62
C(21)	-0.20	-0.20	-0.21	-0.24	-0.24	-0.24	-0.49	-0.49	-0.48	-0.63	-0.63	-0.64
C(22)	-0.21	-0.21	-0.21	-0.26	-0.26	-0.26	-0.52	-0.51	-0.51	-0.65	-0.64	-0.63
C(10)	0.26	0.31	0.32	0.10	0.03	0.01	-0.24	-0.07	0.03	-0.32	-0.18	-0.07
C(20)	0.27	0.31	0.33	0.10	0.04	0.01	-0.24	-0.06	0.03	-0.32	-0.17	-0.06

Table 4. The geometry parameters for *cis*- and *trans*-isomers of BDMA, BDPA, and BDBA from the MNDO, AM1, and PM3 calculations. The values in parenthesis represent geometry parameters for trans-isomers

4. 1). $[\{AlMe_2(NHMe)\}_2]$; *cis*-isomer(C_{2v}), *trans*-isomer(C_{2h})

Distances (Å)	PM3	AM1	MNDO
Al(1)-N(1)	1.884 (1.884)	1.830 (1.830)	1.929 (1.929)
Al(1)-N(2)			
Al(2)-N(1)			
Al(2)-N(2)			
Al(1)-C(11)	1.968 (1.974)	1.805 (1.805)	1.853 (1.854)
Al(1)-C(12)	1.981 (1.974)	1.805 (1.805)	1.855 (1.854)
Al(2)-C(21)			
Al(2)-C(22)			
N(1)-C(10)	1.461 (1.461)	1.444 (1.444)	1.472 (1.472)
N(2)-C(20)			
Angles (°)			
N(1)-Al(1)-N(2)	90.2 (90.1)	89.3 (89.3)	85.0 (85.1)
Al(1)-N(1)-Al(2)	89.8 (89.9)	90.7 (90.7)	94.8 (94.9)
C(11)-Al(1)-N(1)	119.0 (118.5)	113.9 (113.1)	115.3 (115.7)
C(12)-Al(1)-N(1)	119.0 (113.2)	109.8 (110.3)	111.3 (111.0)
C(11)-Al(1)-N(2)			
C(12)-Al(1)-N(2)			
C(10)-N(1)-Al(1)	101.9 (101.8)	115.8 (115.6)	119.9 (119.9)
C(10)-N(1)-Al(2)	101.9 (101.8)	116.2 (115.6)	119.9 (119.9)

4. 2). $[\{AlMe_2(NH^iPr)\}_2]$; *cis*-isomer(C_{2v}), trans-isomer(C_{2h})

Distances (Å)	Expl.[14]	PM3	AM1	MNDO
Al(1)-N(1)	1.953(1.952)	1.888(1.886)	1.834(1.833)	1.940(1.939)
Al(1)-N(2)	1.936(1.965)			
Al(2)-N(1)	1.956			
Al(2)-N(2)	1.950			
Al(1)-C(11)	1.940(1.962)	1.979(1.982)	1.807(1.808)	1.856(1.858)
Al(1)-C(12)	1.971(1.966)	1.984(1.982)	1.808(1.808)	1.858(1.858)
Al(2)-C(21)	1.962			
Al(2)-C(22)	1.952			
N(1)-C(10)	1.489(1.488)	1.472(1.472)	1.465(1.465)	1.489(1.489)
N(2)-C(20)	1.514			
C(10)-C(101)	1.504(1.513)	1.531(1.531)	1.533(1.532)	1.552(1.552)
C(10)-C(102)	1.515(1.525)			
C(20)-C(201)	1.469			
C(20)-C(202)	1.533			
Angles (°)				
N(1)-Al(1)-N(2)	87.4(89.2)	88.4(90.3)	88.9(89.2)	85.4 (86.5)
Al(1)-N(1)-Al(2)	91.5 (90.8)	89.3 (89.7)	90.4(90.8)	92.8(93.5)
C(11)-Al(1)-N(1)	111.9(112.5)	120.4(122.7)	114.6(115.7)	114.9(117.0)
C(12)-Al(1)-N(1)	111.2(108.3)	112.1(109.0)	109.7(108.6)	111.1(108.9)
C(11)-Al(1)-N(2)	111.4(108.6)			
C(12)-Al(1)-N(2)	109.8(113.3)			
C(10)-N(1)-Al(1)	119.2(120.6)	104.4(104.5)	117.0(117.7)	122.2(122.3)
C(10)-N(1)-Al(2)	121.5(121.3)			
C(101)-C(10)-C(102)	110.8(110.9)	109.9(109.3)	107.7(108.1)	109.8(109.7)
C(101)-C(10)-N(1)	110.8(111.1)	111.5(111.5)	113.0(112.9)	112.6(112.7)
C(102)-C(10)-N(1)	110.7(110.7)			

4. 3). $[\{AlMe_2(NH^tBu)\}_2]$; *cis*-isomer(C_{2v}), *trans*-isomer(C_{2h})

Distances (Å)	PM3[a]	AM1	MNDO
Al(1)-N(1)	1.879 (1.877)	1.838 (1.837)	1.950 (1.948)
Al(1)-N(2)	1.998 (1.996)	1.837 (1.837)	1.950 (1.948)
Al(2)-N(1)			
Al(2)-N(2)			
Al(1)-C(11)	1.978 (1.977)	1.807 (1.810)	1.853 (1.859)
Al(1)-C(12)	1.979 (1.981)	1.816 (1.810)	1.864 (1.859)
Al(2)-C(21)			
Al(2)-C(22)			
N(1)-C(10)	1.510 (1.509)	1.479 (1.480)	1.503 (1.503)
N(2)-C(20)			
C(10)-C(101)	1.543 (1.542)	1.542 (1.534)	1.567 (1.557)
C(10)-C(102)	1.541 (1.541)	1.544 (1.543)	1.567 (1.566)
C(10)-C(103)	1.534 (1.534)	1.544 (1.543)	1.567 (1.566)
C(20)-C(201)			
C(20)-C(202)			
C(20)-C(203)			
Angles (°)			
N(1)-Al(1)-N(2)	89.2 (89.8)	89.3 (88.9)	85.4 (85.9)
Al(1)-N(1)-Al(2)	89.4 (90.2)	90.6 (91.1)	93.5 (94.1)
C(11)-Al(1)-N(1)	125.9 (125.9)	120.3 (119.4)	118.1 (119.2)
C(12)-Al(1)-N(1)	115.8 (116.4)	106.6 (107.5)	109.6 (108.8)
C(11)-Al(1)-N(2)	109.7 (112.8)		
C(12)-Al(1)-N(2)	105.1 (100.5)		
C(10)-N(1)-Al(1)	102.2 (102.3)	122.1 (122.8)	126.5 (126.2)
C(10)-N(1)-Al(2)	137.4 (137.7)	122.3 (122.8)	126.5 (126.2)
C(103)-C(10)-N(1)	113.1 (110.0)	113.3 (114.1)	112.6 (112.3)

[a] PM3 method gives C_2 and C_1 point group for *cis*- and *trans*-isomer, respectively.

PM3 calculations increase by 0.014 Å, 0.014 Å, and 0.038 Å, respectively, when the R group is changed from ^{i}Pr to ^{t}Bu. The increase of the N-C bond lengths can be interpreted as the weakening of the N-C bond, thus shows the same tendency as the experimental deposition temperature. It is, however, not in line with the N-C ROPs for the constrained geometry that show the insignificant change in the MNDO, AM1, and PM3 calculations and the significant change in the ASED-MO calculation. Thus, it suggests that the steric effect of R groups may be more important than the electronic effect of R groups for the decomposition of N-C bonds.

The difference in the heat of formation between *trans*- and *cis*-isomers represents the relative stability among the BDMA, BDPA, and BDBA. In the MNDO, AM1, and PM3 calculations the relative stability between *trans*- and *cis*-isomers in BDBA is just the same as in the NMR results[27] for which the ratio of *trans*- to *cis*-BDBA is 2 : 1. In the NMR experiment, the net enthalpy change from *trans*-isomer to *cis*-isomer of BDBA in the isomerization process is 0.53 ± 0.02 kcal/mol. This experimental value is in good agreement with the MNDO result of 0.75 kcal/mol and the PM3 result of 0.45 kcal/mol. The relative stability of *cis*-isomer to *trans*-isomer of BDPA isomers from calculations does not agree with the NMR and X-ray study[14] in which the ratio of *cis* to *trans* isomers is close to 2 : 1. PM3 and AM1 calculations indicate that trans isomer of BDPA is

more stable than *cis*-BDPA while both isomers have about the same energy in the MNDO calculation. It appears that the calculated stabilities have only limited reliability for these compounds since the energy differences are typically less than 1.0 kcal/mol.

Conclusions

In an effort to identify better precursors for use in synthesizing high quality AlN thin films, we have carried out theoretical investigations of the electronic properties and atomic structures of the selected organometallic precursors $[Me_2AlNHR]_2$ (R = Me, ^{i}Pr, and ^{t}Bu) by using the ASED-MO, MNDO, AM1, and PM3 semiempirical methods. The following principal conclusions are derived from the present work:

1. The N-C reduced overlap population data suggest that on electronic grounds these bonds should strengthen in the order of substituents Me- < ^{i}Pr- < ^{t}Bu- from the ASED-MO calculations, but be little affected by the substituents from the MNDO, AM1, and PM3 calculations. But as the R group is changed for the precursors, the optimized N-C bond lengths calculated at the MNDO, AM1, and PM3 levels increase in the order: BDMA < BDPA < BDBA. Clearly the steric effects will contribute to the opposite trend, as exemplified by the semi-empirically optimized structures. This steric effect correlates best with the experimental deposition temperatures of 770 K for BDPA and 720 K for BDBA.[21]

2. The differences in bond lengths between *cis*- and *trans*-isomers in the MNDO, AM1, and PM3 calculations are insignificant in all the precursors considered.

Therefore, our results suggest that C-N fission may be an important step in forming AlN films from the organometallic precursors, since tendency of the experimental deposition temperature for the film formation agrees best with the variation of bond lengths of the C-N bonds in the bulky order of alkyl substituents. The C-N bond lengths of AlN precursors calculated by MNDO, AM1, and PM3 methods could be useful in screening of precursors.

Acknowledgment. We thank the reviewers for the very valuable comments. The present studies (K. H. L.) were supported in part by the Basic Science Research Institute Program, Ministry of Education 1997, Project No. 97-3438 and the KOSEF 90-03-00-03. The work (Y. S. L. and S. K.) was partially supported by the Korea Science and Engineering Foundations through the Center for Molecular Science at the KAIST. Y. K. acknowledges financial support by the Ministry of Science and Technology.

References

1. Kurokawa, Y.; Utsumi, K.; Takamizawa, H.; Kamata, T.; Noguchi, S. *IEEE Trans. On Components, Hybrids, and Manufacturing Tech. CHMT.* **1985**, *8*, 247.
2. CRC Handbook of Chemistry and Physics, 59th ed.; Weast, R. C., Ed.; CRC Press: Inc.; Florida 1978.
3. Perry, P. B.; Rutz, R. F. *Appl. Phys. Lett.* **1978**, *33*, 319.
4. Yim, W. M.; Stofko, E. J.; Zanzucchi, P. J.; Pankove, J. I.; Ettenberg, M.; Gilbert, S. L. *J. Appl. Phys.* **1973**, *44*, 292.
5. Gautier, M.; Duraud, J. P.; Le Gressus, C. *Surface Sci.* **1986**, *178*, 201.
6. Li, X.; Zuchuan, X.; Ziyou, H.; Huazhe, C.; Wuda, S.; Zhongcai, C.; Feng, Z.; Enguang, W. *Thin Solid Films* **1986**, *139*, 261.
7. Gabe, E.; Le Page, Y. *Phys. Rev.* **1981**, *B24*, 5634.
8. Kobayashi, A.; Sankey, O. F.; Volz, S. M.; Dow, J. D. *Phys. Rev.* **1983**, *B28*, 935.
9. Olson, C. G.; Sexton, J. H.; Lynch, D. W.; Bevolo, A. J.; Shanks, H. R.; Harmon, B. N.; Ching, W. Y.; Wieliczka, D. M. *Solid State Commun.* **1985**, *56*, 35.
10. Awad, M. K.; Anderson, A. B. *Surface Sci.* **1989**, *218*, 543.
11. (a) Mayer, T. M.; Rogers Jr., J. W.; Michalske, T. A. *Chem. Mater.* **1991**, *3*, 641. (b) Bartram, M. E.; Michalcke, T. A.; Rogers, Jr., J. W.; Mayer, T. M. *Chem. Mater.* **1991**, *3*, 953. (c) Gaskill, D. K.; Bottka, N.; Lin, M. C. *J. Cryst. Growth* **1986**, *77*, 418.
12. (a) Zanella, P.; Rossetto, G.; Brianese, N.; Ossola, F.; Porchia, M.; Williams, J. O. *Chem. Mater.* **1991**, *3*, 225. (b) Ho, K. L.; Jensen, K. F. *J. Cryst. Growth* **1991**, *107*, 376.
13. (a) Bowen, R. E.; Gosling, K. *J. Chem. Soc., Dalton Trans.* **1974**, 964. (b) Amirkhalili, S.; Hitchcock, P. B.; Smith, J. D. *J. Chem. Soc., Dalton Trans.* **1979**, 1206.
14. Amirkhalili, S.; Hitchcock, P. B.; Jenkins, A. D.; Nyathi, J. Z.; Smith, J. D. *J. Chem. Soc., Dalton Trans.* **1981**, 377.
15. Al-Wassil, A.-A. I.; Hitchcock, P. B.; Sarisaban, S.; Smith, J. D.; Wilson, C. L. *J. Chem. Soc., Dalton Trans.* **1985**, 1929.
16. Haiduc, I.; Sowerby, D. B. *The Chemistry of Inorganic Homo- and Heterocycles*, Vol. 1 (Academic Press, London, 1987).
17. (a) Sauls, F. C.; Interrante, L. V.; Jiang, Z. *Inorg. Chem.* **1990**, *29*, 2989. (b) Interrante, L. V.; Carpemter II, L. E.; Whitmarsh, C.; Lee, W.; Garbauskas, M.; Slack, G. A. *Mat. Res. Soc. Symp. Proc.* **1986**, *73*, 359.
18. Interrante, L. V.; Lee, W.; McConnell, M.; Lewis, N.; Hall, E. *J. Electrochem. Soc.* **1989**, *136*, 472 and references therein.
19. Boyd, D. C.; Haasch, R. T.; Mantell, D. R.; Schulze, R. K.; Evans, J. F.; Gladfelter, W. T. *Chem. Mater.* **1989**, *1*, 119.
20. (a) Park, J. T.; Lee, J.-K.; Kim, S.; Sung, M. M.; Kim, Y. *Bull. Korean Chem. Soc.* **1993**, *14*, 163 and references therein. (b) Park, S. M.; Boo, B. H.; Kim, Y.; Park, J. T.; Koyano, I. *Jpn. J. Appl. Phys.* **1995**, *34*, L933.
21. Sung, M. M.; Jung, H. D.; Lee, J.-K.; Kim, S.; Park, J. T.; Kim, Y. *Bull. Korean Chem. Soc.* **1994**, *15*, 79.
22. (a) Anderson, A. B. *J. Chem. Phys.* **1975**, *62*, 1187. (b) Brock, C. P.; Companion, A. L.; Kock, L. D.; Niedenzu, K. *Inorg. Chem.* **1991**, *30*, 784.
23. (a) Anderson, A. B.; Grimes, R. W.; Hong, S. Y. *J. Phys. Chem.* **1987**, *91*, 4245. (b) Chu, S.-Y.; Anderson, A. B. *Surface Sci.* **1988**, *194*, 55. (c) Anderson, A. B. *Phys. Rev.* **1973**, *B8*, 3824.
24. Ling, Y.; Xide, X. *Surface Sci.* **1991**, *247*, L204.
25. MOPAC93, J. J. P. Stewart, Fujitsu Limited, Tokyo, Japan (1993).
26. $\text{Percent} = \frac{\text{ROP of BDPA (or BDBA)} - \text{ROP of BDMA}}{\text{ROP of BDMA}} \times 100$
27. Park, J. T.; Oh, W. T.; Kim, Y. *Bull. Korean Chem. Soc.* **1996**, *17*, 1147.